Journal of Materials Chemistry C

ROYAL SOCIETY OF CHEMISTRY

PAPER

View Article Online
View Journal | View Issue

Cite this: J. Mater. Chem. C, 2020, 8, 6914

Optically and electrically modulated printed carbon nanotube synaptic transistors with a single input terminal and multi-functional output characteristics†

Lin Shao,‡[a] Min Li,‡[ab] Peisong Wu,[c] Fang Wang,[c] Shulin Chen,[a] Weida Hu,[c] Hua Wang,*[b] Zheng Cui*[a] and Jianwen Zhao*[a]

Received 5th March 2020,
Accepted 14th April 2020

DOI: 10.1039/d0tc01156h

rsc.li/materials-c

The development of new and multi-functional synaptic transistors has become a research highlight in brain science and brain-like intelligence technologies. Here, we report an optically and electrically modulated carbon nanotube synaptic transistor with a single input terminal and multi-functional output characteristics. The optoelectronic response characteristics of carbon nanotube synaptic transistors can be controlled by the pulsed optical and electrical signals *via* a lightly doped silicon gate electrode as the input terminal. Some important synaptic behaviors including low-pass filtering and non-volatile memory performance were investigated after training by pulsed light and/or voltage stimulations. High neural activities with multiple input and output performances, such as excitatory, inhibitory and logic behaviour (NOR logic gate), were also observed by simultaneously programming the optical and electrical stimulations. As far as we know, this is the first report of a printed carbon nanotube synaptic transistor with a single gate electrode that has the ability to concurrently receive pulsed electrical and optical inputs as well as to realize multi-functional outputs. The results provide an opportunity for the coupling of multiple inputs through different stimulation methods in emerging brain-like synaptic nanoelectronics.

1. Introduction

The human brain can efficiently process and store a variety of information received from different pathways including olfactory, perception, hearing, vision, motion, *etc.* However, it is a challenge for super-fast computers to realize these functions as efficiently as a human brain with only low power dissipation. The human brain has about 10^{11} neurons and every neuron links together with more than a thousand synapses, which forms a complex information processing neural network.[1–3] Therefore, hardware-based synapses/neurons utilizing electronic/ionic hybrid devices are a promising way to realize brain-like recognition and computing. To date, three-terminal transistors, *e.g.* organic semiconductor transistors,[4–7] two-dimensional (2D) material transistors,[8–10] metal oxide-based transistors[11–17] and carbon nanotube transistors[18,19] have been proposed for artificial synapses and neuromorphic systems.[20–24] Synaptic transistors with multi-terminals[25] can receive signals from many sources at the same time, and can therefore exhibit spatiotemporal effects. Additionally, they can simultaneously receive and read stimuli to simulate higher neural activities and more complicated logic functions.[26] Therefore, most of these synaptic transistor devices with multi-terminals are regarded as the information processing units.[14] Among them, optical synaptic transistor devices are becoming increasingly

[a] Printable Electronics Research Centre, Suzhou Institute of Nano-Tech and Nano-Bionics, Chinese Academy of Sciences, 398 Ruoshui Road, Suzhou 215123, P. R. China. E-mail: jwzhao2011@sinano.ac.cn, zcui2009@sinano.ac.cn; Fax: +86-512-62603079; Tel: +86-512-62872705

[b] Key Laboratory of Interface Science and Engineering in Advanced Materials of Ministry of Education, Taiyuan University of Technology, No. 79, Yingze West Main Street, Taiyuan, 030024, P. R. China. E-mail: wanghua001@tyut.edu.cn

[c] State Key Laboratory of Infrared Physics Shanghai Institute of Technical Physics, Chinese Academy of Sciences, 500 Yutian Road, Shanghai 200083, P. R. China

† Electronic supplementary information (ESI) available: Fig. S1–S5 as described in the text, amplitude of EPSC increases gradually with the successive pulsed voltage stimulus for the phosphorous-doped silicon gate synaptic transistor device (from 2 to 1.6 V), and the light-response performance and the changes of EPSC of a printed carbon nanotube transistor device with different stimulation cycles under different atmospheric conditions (Fig. S1); schematic illustrations of carrier distributions in lightly boron-doped silicon and photogating effects at the interface between silicon and HfO_2 under pulsed light illumination or gate voltage stimulation (Fig. S2); (a) transfer curves and (b) I_D – time curves of the transistor device under the light and dark conditions (Fig. S3); the changes of EPSC under different (a) gate voltage and (b) light pulse frequency (Fig. S4); "NOR" logic operation using only one bottom gate with 40 pulse sequence (Fig. S5). See DOI: 10.1039/d0tc01156h

‡ Lin Shao and Min Li contributed equally to this paper.

important since they can be used to mimic the visual systems of the brain with a large bandwidth, low interconnection energy loss and ultrafast signal transmission. Optically modulated synaptic devices can be used to develop novel bioinspired electronic devices with optical wireless communications. In some way, these optical synaptic transistor devices can compensate for the deficiency of electrically stimulated synaptic transistor devices, whose area can be made smaller by controlling the wavelength of light without increasing the input gates.[27–29] However, the development of optical synaptic transistor devices still lags far behind electrically stimulated synaptic transistors. Up to now, there have been few reports about single-gate synaptic transistors with multiple input signals and output characteristics, and these synaptic transistors with single-gate electrodes cannot receive signals from both the pulsed light and electrical stimulations, nor can they mimic higher neural activities including excitatory, inhibitory and logic functions.

In this work, we report electrically and optically controllable carbon nanotube synaptic transistors with a single silicon bottom gate electrode. We found that our printed carbon nanotube synaptic transistors exhibit both positive and negative responses to the pulsed optical stimulation signals when using the lightly boron-doped (p-type) and phosphorous-doped (n-type) silicon gate electrodes as input terminals, respectively. Several important synaptic behaviors including low-pass filtering and non-volatile memory performance have been successfully imitated under the pulsed light and voltage stimulations. The results demonstrate that the memory ability increased with the increase in stimulation time. The memory retention time of synaptic transistors could be up to 3600 s, when trained by the pulsed optical or electric signals more than 200 times. Furthermore, the significant biological synapse performances, such as spatiotemporally correlated dynamic logic (NOR logic function), excitatory and inhibitory behaviours, were successfully emulated by concurrently programming the light and voltage stimulations. This is a promising approach to coupling with multiple inputs and outputs with complicated neural functions through various stimulation methods in a brain-like synaptic transistor.

2. Experimental section

To achieve printable semiconducting single-walled carbon nanotube (sc-SWCNT) inks, 3 mg of P-DPPb5T (poly-diketopyrrolopyrrole 5-thiophene) or 3 mg PFIID (isoindigo-based poly(9,9-dioctylfluorene)) was dissolved in 10 mL toluene, and then 5 mg of SWCNTs (purchased from Carbon Solutions, USA, with a diameter of ~1.2–1.6 nm and a length of ~1–1.6 μm) were added into as-prepared polymer solutions. The mixtures were then sonicated for 30 min in an ice water bath (0 °C). Subsequently, the resulting suspensions were centrifuged at 30 000 g for 1 h to obtain sc-SWCNT inks with few-bundle or individual carbon nanotubes. Absorption spectra of the supernatant were characterized by a Lambda 750 UV/Vis/NIR spectrometer from PerkinElmer, Inc., USA. The supernatant was used to construct carbon nanotube transistors and synaptic transistor devices *via* aerosol jet printing, and the morphology of the carbon nanotube films in the device channels were characterized by a Hitachi S-4800 scanning electron microscope. The device fabrication process and measurements are reported elsewhere.[30–32] The fabrication process of printed SWCNT TFT devices is as follows: 50 nm thick HfO_2 or Al_2O_3 thin films were deposited on lightly doped silicon substrates (the electrical resistivities of lightly p-doped and n-doped silicons are 20–30 and 14–16 Ω cm, which were purchased from Zhejiang Lijing Silicon Material Co., Ltd) at 250 °C using the atomic layer deposition (ALD) technique. Subsequently, prepatterned interdigitated Au/Ti (50 nm Au/5 nm Ti) electrode arrays were fabricated on the 50 nm HfO_2/Si or Al_2O_3/Si substrates by photolithography, e-beam deposition, and lift-off process (the channel width, length, and interdigital electrode space are 1000, 20, and 20 μm, respectively.). After that, the substrates were treated by oxygen plasma (100 W) for 3 min, and then sc-SWCNT inks were printed into the device channels by the Aerosol Jet printer, followed by washing with toluene. Finally, the devices were annealed on the hot plate at 120 °C for 30 min. Here, we focused on studying the performance of the optically and electrically modulated carbon nanotube synaptic transistor devices using lightly boron-doped (p-type) silicon as the bottom gates in this work. To study the performance of synaptic transistor devices, we used a 532 nm laser (purchased from Changchun New Industries Optoelectronics Tech. Co) as the light source to stimulate the printed carbon nanotube transistor devices.

3. Results and discussion

3.1. Electric properties of as-prepared printed carbon nanotube transistors

Construction of printed carbon nanotube transistors with high on/off ratios and high mobility requires well-dispersed few-bundle or individual semiconducting carbon nanotubes in sorted sc-SWCNT inks. Absorption spectra of sc-SWCNT inks sorted by PFIID and P-DPPb5T, and the typical morphology of a carbon nanotube film in the printed carbon nanotube transistor device channels are illustrated in Fig. 1a and b. We can see from Fig. 1a and b that sorted sc-SWCNTs by PFIID and P-DPPb5T dispersed well after sonication and high-speed centrifugation at 30 000 g for 1 h, and few-bundle and individual nanotubes with high density were observed in device channels.

Fig. 2a is the schematic of an optically and electrically controllable carbon nanotube synaptic transistor device under pulsed light and/or voltage stimulation. Fig. 2b is the typical transfer curve of a synaptic transistor with lightly doped silicon as the bottom gate, which displays electrical properties similar to the previously reported carbon nanotube transistors.[30–33] Printed carbon nanotube transistor devices exhibit p-type characteristics, with low leakage current (~0.022 nA), high on/off ratio (10^6), good mobility (~12 $cm^2\ V^{-1}\ s^{-1}$) and small subthreshold swing (129 mV per decade) at gate voltages from −2 to 2 V. The amplitude of drain current for all lightly (boron and phosphorous) doped silicon gate devices gradually increases

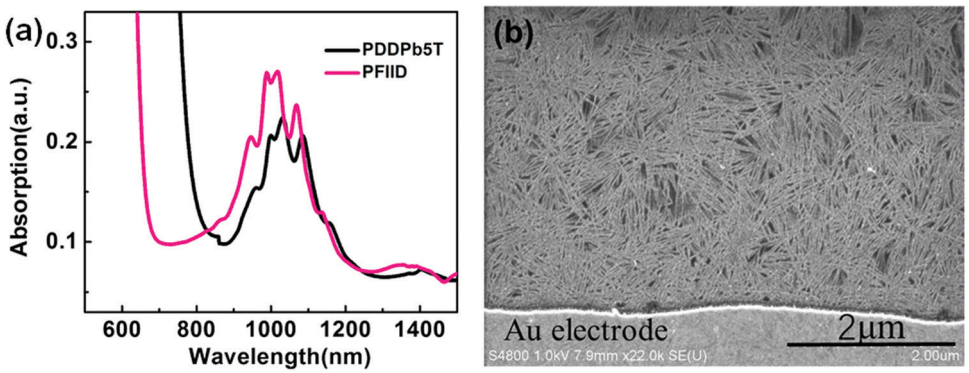

Fig. 1 (a) The absorption spectra of the sorted sc-SWCNT inks by PFIID and PDPPb5T, and (b) the typical morphology of a printed sc-SWCNT thin film in the printed carbon nanotube transistor device channel.

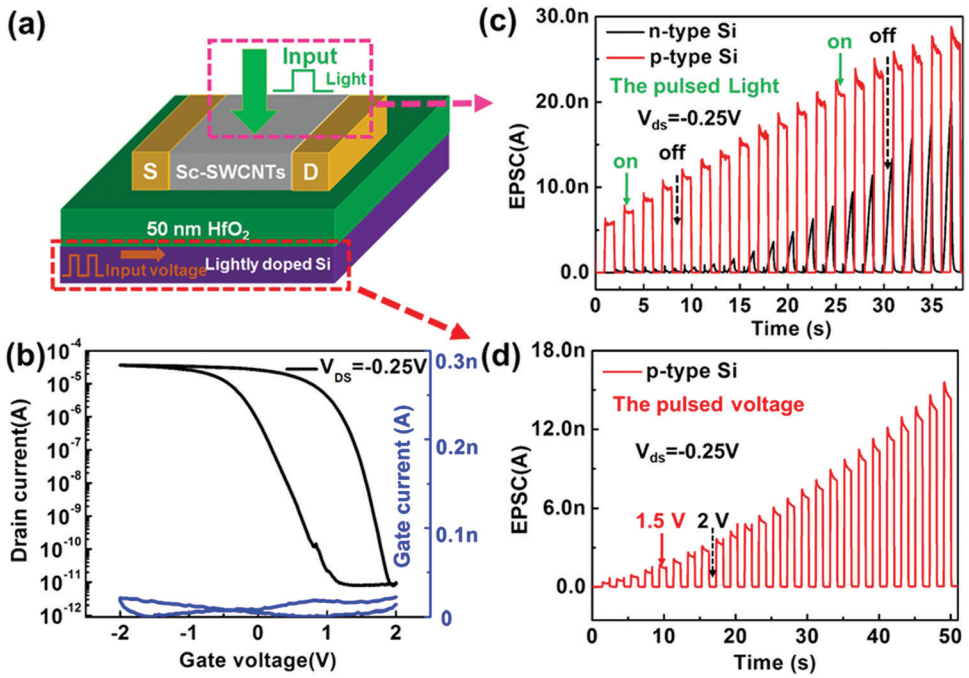

Fig. 2 (a) Schematic and (b) typical transfer curve of an optically and electrically controllable carbon nanotube synaptic transistor device. EPSCs recorded for pre-synaptic pulsed sequences (f = 0.5 Hz). The amplitude of EPSC increases step by step with the continuous pulsed sequences (c) light (the light power is 50 mW, and the gate voltage and V_{DS} is 2 and −0.25 V) and (d) gate voltage stimulus (from 2 to 1.5 V) with V_{DS} of −0.25 V. Source and drain electrodes are Au/Ti (50 nm Au/5 nm Ti) electrodes, and the channel length is 20 μm.

with a series of pre-synaptic pulsed light and voltage stimulations (V_{DS} = −0.25 V, and f = 0.5 Hz) as shown in Fig. 2c, d and Fig. S1a (ESI†), which looks like the biological synapse functions of learning and memory. Excitatory post-synaptic currents (EPSCs) or inhibitory post-synaptic currents in a post-synaptic neuron are triggered by the pulsed signals from pre-synaptic neurons because the biological short-term facilitation reflects an increase in the neurotransmitter release that lasts for up to hundreds of milliseconds, induced by the accumulation of the calcium in the pre-synaptic terminal.[34] Our transistors showed the ability to imitate the synapse functions when the pulsed optical and electrical signals were applied on the lightly doped silicon (called the pre-synaptic input terminal), and the drain current is called EPSC. Charge carriers are gradually accumulated in the carbon nanotube/HfO_2 interface by the positive pre-synaptic spike due to the existence of some trapping states in carbon nanotube transistor channels.[30,35] It should be noted that the charge trapping, which gives rise to the increasing current, is purposely achieved by limiting the gate switching voltage between 1.5 and 2 V. The use of a negative/positive gate voltage results in current pulses of constant height. It is noteworthy that synaptic transistors using lightly boron-doped and phosphorous-doped silicon as the input terminals exhibited opposite responses to the pulsed light stimulations (Fig. 2c); *i.e.*, the synaptic transistors with lightly boron-doped and phosphorous-doped silicon gate electrodes showed positive

and negative responses to the pulsed light stimulations due to the induced opposite photovoltages (Fig. 5b),[30] respectively.

To confirm the existence of trapping states in the device channel, EPSCs was performed under different pressures as shown in Fig. S1b (ESI†). It is obvious that EPSC values at the low pressures (10^{-3} and 10^{-5} atm (standard atmospheric pressure) are obviously lower than those at relatively high pressure (1 atm)). It demonstrates that oxygen has a positive effect on the EPSC responses in the synaptic transistors. We speculated that there were some trap states in the device channels due to O_2 adsorbed on the surfaces of sorted sc-SWCNTs and dielectrics. As shown in Fig. S2 (ESI†), there are more trap states in the interfaces and on the surfaces of the printed transistor in the atmosphere, and more induced negative charges (such as O^{2-} or electrons) are captured in the channels of printed transistors when stimulated by the same pulsed optical signals. The negative charges generate a gating effect, which is helpful to trigger the hole injection from the source electrode to the device channel.[36] At the same time, a negative photovoltage is formed at the lightly boron-doped silicon bottom gate. Thus, the concentrations of holes in the synaptic transistor device rapidly increases, resulting in the abrupt increase of drain currents when the light is turned on.[37] Furthermore, we explored the relationship between the transfer curves and the current changes with time under the light and dark conditions shown in Fig. S3 (ESI†), which further confirmed the accumulation of carriers in the channel under the light illumination. Fig. 2c and d showed the simulated EPSC after 25 spike trainings with a 2500% and 2672% facilitation under the pulsed light and voltage stimulations at 22 Hz, respectively. Therefore, these transistors can be used to study the synaptic characteristics.

3.2. Low-pass filtering performance of printed carbon nanotube synaptic transistors

Climbing fibre synapses have been found to have a high initial probability of release, which can function as low-pass filters at the start of pre-synaptic action in biological synapses. Because the probability of its vesicle release depends on the activity, these types of synapses can imitate dynamic filters for information transmission.[38,39] The vesicle exhibits high activity under low-frequency signal stimulation, *i.e.*, the synapses show the ability to selectively response to a low-frequency pulsed signal. Fig. 3a shows the low-pass filtering characteristics of a synapse. To assess the filtering performance of an optically and electrically controllable carbon nanotube synaptic transistor, EPSCs were measured while a range of pre-synaptic electric and optical pulse sequence at different frequencies were applied to the bottom gate. The amplitudes of EPSC rose gradually with the training of consecutive 25 spike stimulations at a frequency of 0.5 Hz under light or voltage stimuli as shown in Fig. S4a and b (ESI†). Fig. 3b represents the function between the amplitude gains of the spikes and the pulsed frequencies. The amplitude of EPSC increased more rapidly at the frequencies from 0.5 to 10 Hz. For the voltage pulse training frequencies changing from 0.5 to 10 Hz (0.5, 1, 2, 4 and 10), the amplitude gains were 24, 4.2, 0.25, 0.05, and 0.005, respectively. A similar phenomenon was observed with the training of pulsed light stimulation. The amplitude gains were 26.72, 7.85, 2.37, 1.26, and 0.059 at light pulse frequencies of 0.5, 1, 2, 4, and 10 Hz, suggesting the stronger coupling effects under the lower stimulus frequency.

3.3. Non-volatile photoelectric memory of printed carbon nanotube transistors after training

To research the performance of non-volatile photoelectrical memory of printed carbon nanotube synaptic transistors, the synaptic transistors were trained by the repeated pulsed light and gate voltage signals (from 200 to 1600 times) at a frequency of 22 Hz as shown in Fig. 4a and c. The EPSCs (En is the amplitude of EPSC after the electrical stimuli, and Pn is the amplitude of EPSC after the optical stimuli) were recorded after training with a waiting time of 1, 5, 10, 20, 30 and 60 min, respectively. "*n*" is defined as the waiting time, and "Eo" and "Po" are the original amplitude of drain current before a series of electrical and optical spike training, respectively. Here, En–Eo and Pn–Po are defined as the changes in amplitudes after the training with a series of voltage and light spikes. Fig. 4b shows the relationship between En–Eo, the waiting time and the training times. The En–Eo increased with the ascent of training times with the same waiting time. For instance, E1–Eo were ~3, 6, 12 and 74 nA after voltage spike training 200, 400, 800 and 1600 times, following waiting for 1 min. The En–Eo fell

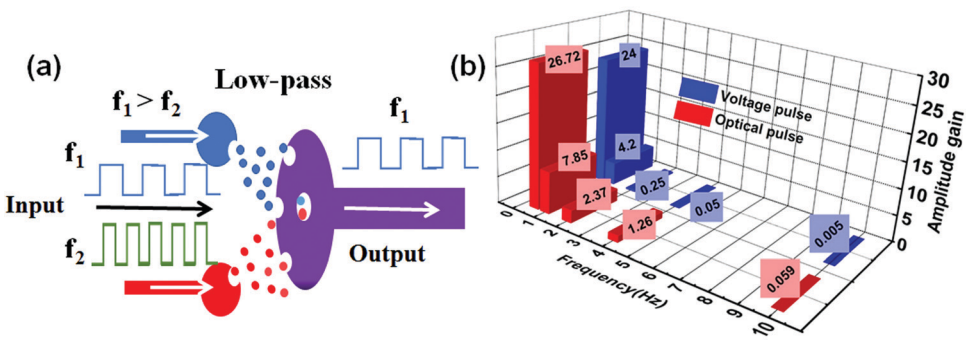

Fig. 3 (a) Schematic of a low-pass filter of a synapse. (b) The relationship between the amplitude gains (called"|A25–A1|/A1") and the pulsed frequencies. A1 and A25 are the EPSC amplitudes of the first and last spike.

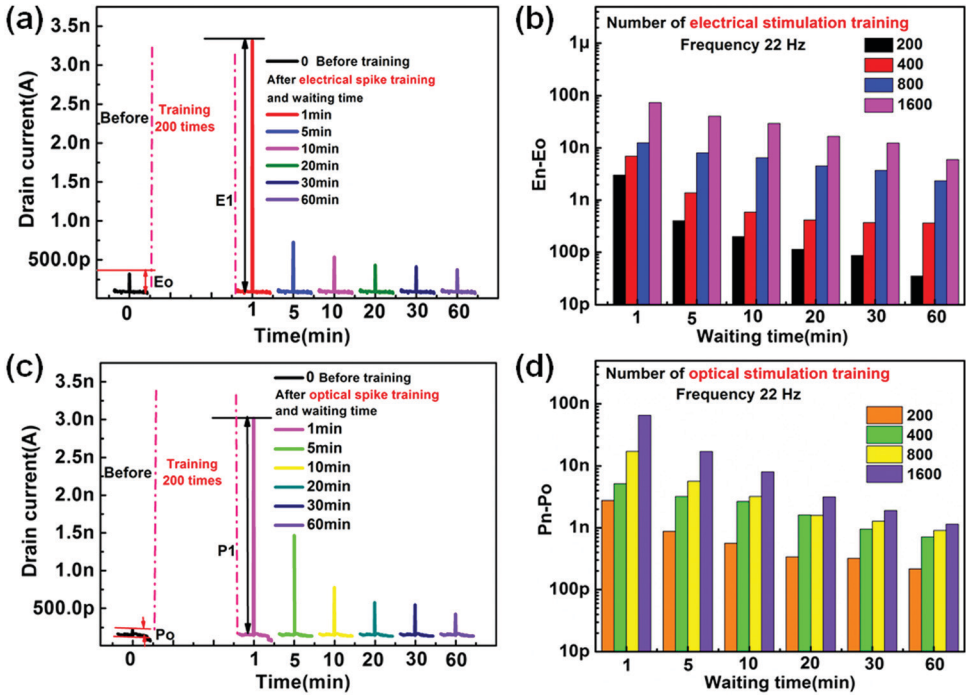

Fig. 4 Performance of the photoelectrical memory based on the printed carbon nanotube transistor. (a) Eo is the amplitude of EPSC at the first pulsed voltage stimulation, and E1 is the EPSC obtained after electrical pulse training 200 times at f = 22 Hz, and then waiting for 1 min in the power-off states. (b) The relationship between En–Eo, the waiting time and the training times after a series of pulsed voltage training. (En–Eo) is the change of amplitude. (c) Po is the amplitude of EPSC at the first pulsed light stimulation before training, and P1 is the EPSC that was obtained after the constant pulsed light training at f = 22 Hz, and then waiting 1 min in the power-off states. (d) The relationship between the amplitude change (Pn–Po), the number of the optical stimulation and the waiting time after ongoing pulsed light training.

with the increase of waiting time after training, and the "memory" was totally removed after 60 min. It is noteworthy that the synaptic transistors were in the power-off state after training by the consecutive pulsed signals, demonstrating that the photoelectric synaptic transistors exhibited good non-volatile and long-term memory.

Similar phenomena were observed under the pulsed optical signals as shown in Fig. 4d. The Pn–Po values increased with the training times under the same waiting time. For instance, P1–Po values were ~65, 17, 8, 3, 2 and 1 nA after training with 1600 optical spikes, following waiting times of 1, 5, 10, 20, 30 and 60 min, respectively, demonstrating that the printed photoelectric synaptic transistors still had good non-volatile and long-term memory after 1600 pulsed light stimulations. However, when the pulse number was 200, the Pn–Po values were ~2.7, 0.9, 0.5, 0.3 and 0.2 nA with waiting times of 1, 5, 10, 20, 30 and 60 min, far below those with 1600 spike stimulation. This was probably attributed to the fact that the trapped charge carriers returned to their initial state after a period of time with the power off. It is apparent that some important synaptic behaviors, such as learning, memory and decay after training, have been successfully imitated after training by the pulsed voltage and light stimualtion.

3.4. Study of the photoelectrical response mechanism

Fig. 5a is the 3D schematic view of a carbon nanotube synaptic transistor under the pulsed optical signal of a 532 nm laser. As reported in previous research,[30] the pulsed light could pass through carbon nanotube thin films and dielectric layers (SiO_2, HfO_2 and Al_2O_3 thin films) and be absorbed by lightly doped silicon substrates, resulting in a voltage at the dielectric/silicon interface. To investigate the photoelectrical response mechanism of the carbon nanotube synaptic transistors, the gate voltages were measured under the training of the pulsed light stimuli as shown in Fig. 5b. The gate voltage showed a sudden decrease after training by the pulsed light. The gate voltages were decreased by ~50 mV (defined as ΔV_{PV}) after every optical pulse due to the photogating effect (light power 50 mW). Concurrently, the baseline of the photovoltages gradually increased with the extended light pulse times because the sustained increase of the induced electrical field (V_{IE}) in lightly boron-doped silicon, and the induced voltage ascended by 0.35 V after training of 20 light spike stimulations. Fig. 5c represents the response rate of a carbon nanotube synaptic transistor under the pulsed optical stimulation. The carbon nanotube transistor showed high response rates to the pulsed light with the rise time and decay time of 0.35 and 2.62 ms, respectively. The I_{off} increased from 10^{-11} to 10^{-9} after training with the pulsed light and/or electrical stimulations along with the positive threshold voltage shift as shown in Fig. 5d, indicating there were some charge carriers produced and stored in the transistor channel after the pulsed light and/or voltage training.

Schematic illustrations of carrier distributions under pulsed light and/or pulsed voltage stimulation are displayed in Fig. S2 (ESI†).

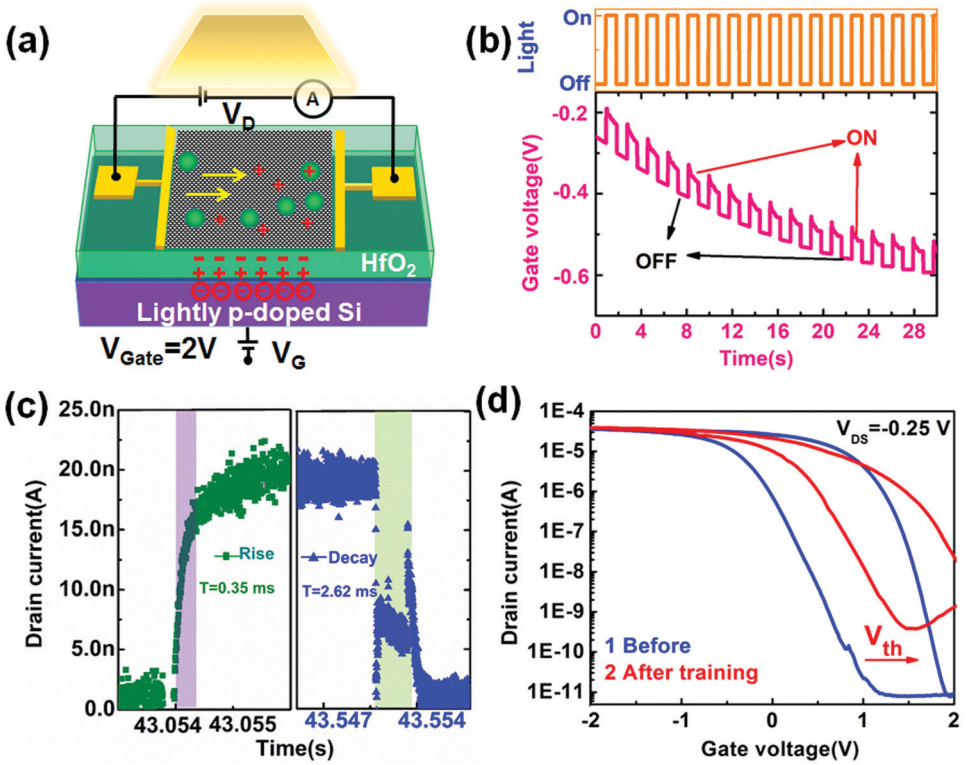

Fig. 5 Light-response performance of the printed synaptic transistors with lightly boron-doped silicon as the gate. (a) Schematic 3D view of a carbon nanotube synaptic transistor device under the pulsed optical signal. (b) The relationship between the gate voltages and the measurement times when the pulsed frequency of the 532 nm laser is 0.5 Hz (the source–drain voltage and the light power are −0.25 V and 50 mW, respectively). (c) Time-dependent photocurrent response, showing the rise time of 0.35 ms and the decay time of 2.62 ms for a carbon nanotube synaptic transistor. (d) The electrical properties of the carbon nanotube synaptic transistor device before and after training by the pulsed light and/or voltage signals.

The synaptic transistor was turned off in the dark at a V_{Gate} of 2 V, and the output drain currents were less than 10^{-9} A, which were calculated by the equation of $|\Delta V_{EV}|\cdot(dI_{DS}/dV_{Gate})$ or $\Delta V_{PV}\cdot(dI_{DS}/dV_{Gate})$, ΔV_{EV} is the change in the gate voltage. It is noted that the synaptic transistor devices were in the off state when monitoring the photoelectrical responses because of the V_{Gate} and V_{DS} of 2 and −0.25 V, respectively. The drain current rapidly increased under the pulsed optical signal (Fig. 2c), suggesting the gate voltages shifted to the negative direction due to the formation of the negative photovoltage from lightly boron-doped silicon ($\Delta V_{PV} < 0$ V) (Fig. S2b, ESI† and Fig. 5b). The drain current droped sharply when the light was turned off *i.e.*, the induced electrical field increased along with the photogating effects disappearing rapidly in the lightly boron-doped silicon, leading to the printed carbon nanotube transistors being totally switched off due to the gate voltage shifting to the positive direction (2 V + ΔV_{IE}) (Fig. S2c, ESI† and Fig. 5b). In other words, printed carbon nanotube transistors would be switched on under pulsed light illumination and switched off completely in the dark. Concurrently, more carriers would be induced and captured in the transistor channel under the pulsed stimulation.[19] As a result, output currents gradually increased with increasing pulse times. As described above, the photoelectrical response mechanism of carbon nanotube synaptic transistors under the pulsed light and/or voltage stimulations can be explained using our previously proposed model.[30]

3.5. Multi-functional output characteristics of printed carbon nanotube synaptic transistors

Although the carbon nanotube transistor has a single gate electrode (lightly boron-doped silicon), it can simultaneously receive the pulsed light and voltage stimulations. We speculate that these kinds of transistors can realize some logic functions and imitate some high neural activities under the pulsed light and voltage simulations. Fig. 2a shows the schematic of a printed carbon nanotube transistor with the simultaneous light and voltage pulses applied to the bottom gate. To ensure that the value of output drain current by the pulsed light was comparable to that by the pulsed voltage stimulation, V_{DS} was fixed at −0.25 V, and the state of light changed from "off" (the power supply was set to 0 V) to "on" (the power supply was set to 5 V) and V_{Gate} was changed from 2 to 1.2 V. In this case, the output currents of the carbon nanotube transistors could be increased by two or three orders of magnitude by the pulsed light or voltage training.

Fig. 6a shows the schematic of a synaptic device based on the printed carbon nanotube transistor under the pulsed light and/or voltage stimulation. An as-prepared synaptic device with a single-gate electrode can realize the "NOR" logic function

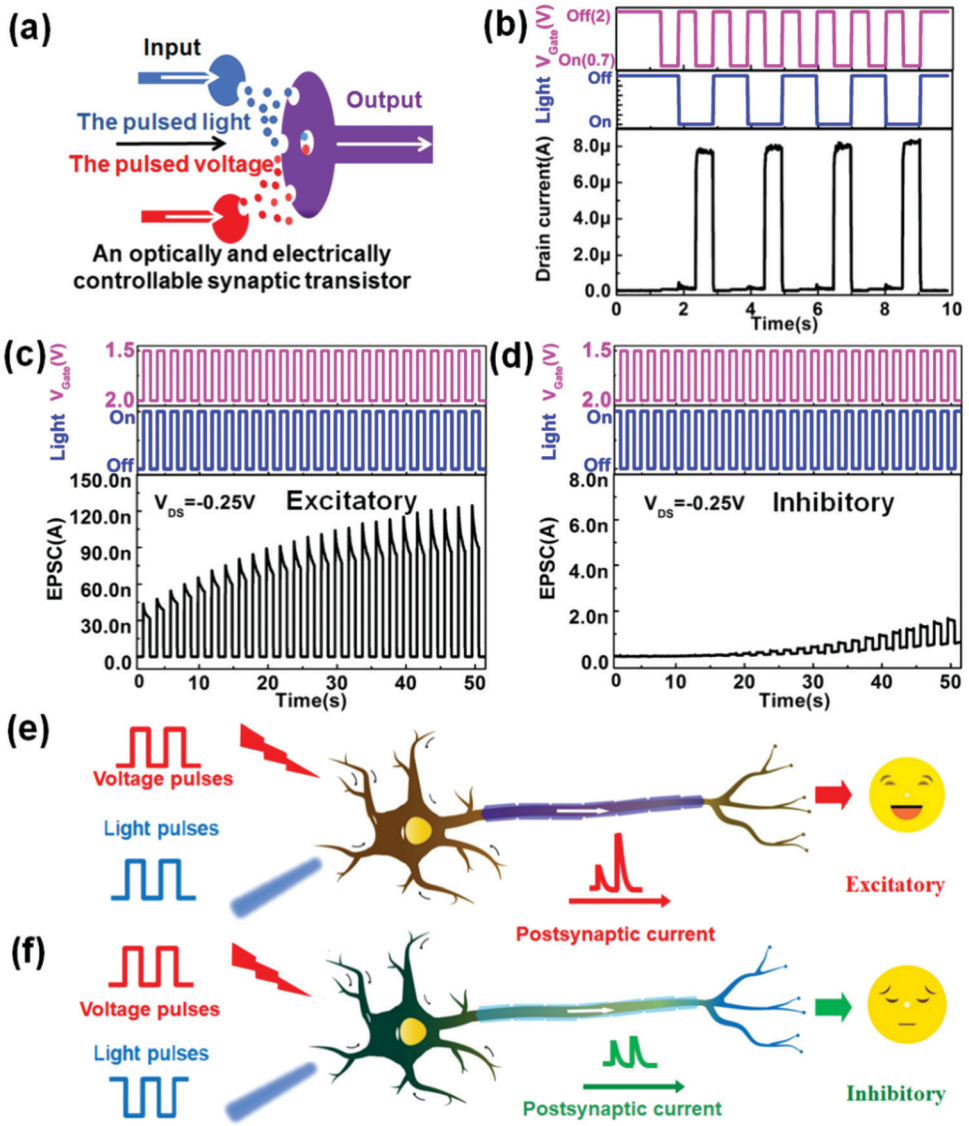

Fig. 6 (a) Schematic of a printed carbon nanotube synaptic transistor under the pulsed light and/or voltage stimulation. (b) NOR logic operation using a single-gate electrode as the input terminal (the laser power of 0.025 mW). Gate voltages of 2.0 (off state) and 0.7 V (on state) are regarded as binary "1" and "0", respectively. The light state is off as "1" and on as "0". (c) EPSC is 126 nA recorded after a pre-synaptic 25 pulse sequence with a frequency of 0.5 Hz. (d) IPSC is 1.6 nA recorded after a pre-synaptic 25 pulse sequence with a frequency of 0.5 Hz. EPSC and IPSC amplitudes increase gradually with the different growth rates because the light pulse program is opposite under the pulsed optical and electrical training. Structure diagrams of the biological synapse of (e) excitatory and (f) inhibitory under the pulsed light and voltage training.

when using light and voltage as input signals, as shown in Fig. 6b. Here, the gate voltages of 2.0 and 0.7 V are called binary "1" (the transistor is in the off-state) and "0" (the transistor is in the on-state). Similarly, "1" for light in the "off state" and "0" for light in the "on state". When the gate voltage is 2.0 V ("1") or the light is in the "off state" ("1"), the drain current is always low ("0"). This means that one input terminal is "1", and the output is always "0". When both light and voltage are in the on state ("0"), the output is "1". This demonstrates that the carbon nanotube synaptic transistor device can perform the "NOR" function when using the pulsed light and voltage as the input signals. At the same time, the output currents marginally increased when increasing the stimulation times as shown in Fig. 6b and Fig. S5a (ESI†). It is interesting to note that the output currents significantly increased with the growth of stimulation times, and the simulated EPSC gradually reached a steady state after about 20 pre-synaptic stimulations, as shown in Fig. S5b (ESI†), when V_{Gate} was changed from 2 to 1.5 V, indicating the balance between the carriers relaxation in the inter-spike gap and the facilitation caused by the next cycle spike.

In a biological synapse, the synaptic weight is consistently weakened or strengthened by information transfer between pre-synaptic and post-synaptic neurons,[40–44] and it can depict different event-dependent synaptic plasticity, which is related to neural activities, such as memory and learning in the human

brain. The variations of synaptic weight resemble excitatory and inhibitory synaptic behaviours in synapses. Here, we call the quick increasing post-synaptic current[45] (PSC) under photoelectric pulse program the ''excitatory PSC'' (EPSC), while the slowly increasing or decreasing PSC value under the pulsed photoelectric training is named the ''inhibitory PSC'' (IPSC). It is noted that the bottom gate of synaptic transistor devices can simultaneously receive optical and electrical pulse signals, which act as axons or dendrites. The EPSC reached 126 nA after a pre-synaptic 25 pulse sequence when the direction of the program was the same between the optical and electrical pulse stimulation, as shown in Fig. 6c, where EPSC was 4 times more than that under the optical or electrical pulse stimuli. This means that the printed carbon nanotube synaptic transistors showed excitatory performances. Nevertheless, the IPSC was only 1.6 nA under the opposite pulse stimuli as shown in Fig. 6d, which was much lower than that under either optical or electrical pulse stimuli after a pre-synaptic 25 pulse sequence (Fig. 2c and d), which is similar to the performance of inhibitory biological synapses. As mentioned above, all our synaptic transistors exhibited a strong optical and electrical coupling effect and could imitate excitatory and inhibitory biological synapses under the pulsed voltage and light stimulations shown in Fig. 6e and f. To sum up, we have presented a novel optical and electrical synaptic transistor device based on printed carbon nanotube transistors whose drain currents can be modulated by pulsed light and voltage *via* the same bottom gate. The optical and electrical tunability of synaptic plasticity demonstrates that our artificial synapses have the capability to imitate a variety of cognitive functions, such as excitatory and inhibitory synapses, logic function and learning.

4. Conclusion

An optically and electrically controllable carbon nanotube synaptic transistor utilizing lightly boron-doped silicon as the bottom gate has been developed. The device can simultaneously receive pulsed electrical and optical inputs, and produce multi-functional outputs. Some important synaptic behaviors (''learning'', ''memory'' and low-pass filtering performance) have been successfully emulated, together with high neural activities (excitatory, inhibitory and NOR logic functions). This work provides a method to combine multiple inputs such as optical and electrical stimulations and demonstrates the potential for parallel processing networks in emerging brain-like synaptic nanoelectronics.

Conflicts of interest

There are no conflicts to declare.

Acknowledgements

Lin Shao and Min Li contributed equally to this work. This work was supported by the Natural Science Foundation of China (61874132), the Key Research Program of Frontier Science of Chinese Academy of Sciences (QYZDB-SSW-SLH031), the National Key Research and Development Program of China (2016YFB0401100), the CAS President's International Fellowship for Postdoctoral Researchers (2019PT0020), the Science and Technology Program of Guangdong Province, China (2016B090906002), the Basic Research Programme of Suzhou Institute of Nano-tech and Nano-bionics (Y5AAY21001), and the Cooperation Project of Vacuum Interconnect Nano X Research Facility (NANO-X) of Suzhou Institute of Nano-tech and Nano-bionics, CAS (H060).

References

1 D. A. Drachman, *Neurology*, 2005, **64**, 2004–2005.
2 J. D. Shepherd and R. L. Huganirl, *Annu. Rev. Cell Dev. Biol.*, 2007, **23**, 613–643.
3 O. Perl, A. Ravia, M. Rubinson, A. Eisen, T. Soroka, N. Mor, L. Secundo and N. Sobel, *Nature Human Behaviour*, 2019, **3**, 501–512.
4 P. Gkoupidenis, N. Schaefer, X. Strakosas, J. A. Fairfield and G. G. Malliaras, *Appl. Phys. Lett.*, 2015, **107**, 1156–1157.
5 E. J. Kim, K. A. Kim and S. M. Yoon, *J. Phys. D: Appl. Phys.*, 2016, **49**, 075105.
6 Y. Lee and T. W. Lee, *Acc. Chem. Res.*, 2019, **52**, 964–974.
7 S. Li, F. Zeng, C. Chen, H. Liu, G. Tang, S. Gao, C. Song, Y. Lin, F. Pan and G. Dong, *J. Mater. Chem. C*, 2013, **1**, 5292–5298.
8 H. Tian, W. Mi, X. F. Wang, H. Zhao, Q. Y. Xie, C. Li, Y. X. Li, Y. Yang and T. L. Ren, *Nano Lett.*, 2015, **15**, 8013–8019.
9 L. Sun, Y. Zhang, G. Hwang, J. Jiang, D. Kim, Y. A. Eshete, R. Zhao and H. Yang, *Nano Lett.*, 2018, **18**, 3229–3234.
10 S. Seo, S. H. Jo, S. Kim, J. Shim, S. Oh, J. H. Kim, K. Heo, J. W. Choi, C. Choi, D. Kuzum, H. S. Philip Wong and J.-H. Park, *Nat. Commun.*, 2018, **9**, 5106.
11 R. A. John, J. Ko, M. R. Kulkarni, N. Tiwari, C. Nguyen Anh, N. G. Ing, W. L. Leong and N. Mathews, *Small*, 2017, **13**, 1701193.
12 X. Wan, Y. Yang, P. Feng, Y. Shi and Q. Wan, *IEEE Electron. Dev. Lett.*, 2016, **37**, 299–302.
13 G. Gou, J. Sun, C. Qian, Y. He, L. Kong, Y. Fu, G. Dai, J. Yang and Y. Gao, *J. Mater. Chem. C*, 2016, **4**, 11110–11117.
14 Y. He, Y. Yang, S. Nie, R. Liu and Q. Wan, *J. Mater. Chem. C*, 2018, **6**, 5336–5352.
15 J. Li, Y.-H. Yang, Q. Chen, W.-Q. Zhu and J.-H. Zhang, *J. Mater. Chem. C*, 2020, **8**, 4065–4072.
16 Y. Guo, L. Q. Zhu, T. Y. Long, D. Y. Wan and Z. Y. Ren, *J. Mater. Chem. C*, 2020, **8**, 2780.
17 S. Kim, S. Kim, J. Park, G. Kim, J. Park, K. C. Saraswat, J. Kim and H. Yu, *ACS Nano*, 2019, **13**, 10294–10300.
18 C. J. Wan, Y. H. Liu, P. Feng, W. Wang, L. Q. Zhu, Z. P. Liu, Y. Shi and Q. Wan, *Adv. Mater.*, 2016, **28**, 5878–5885.
19 P. Feng, W. Xu, Y. Yang, X. Wan, Y. Shi, Q. Wan, J. Zhao and Z. Cui, *Adv. Funct. Mater.*, 2017, **27**, 1604447.

20 J. Shi, S. D. Ha, Y. Zhou, F. Schoofs and S. Ramanathan, *Nat. Commun.*, 2013, **4**, 2676.
21 K. Kim, C. L. Chen, Q. Truong, A. M. Shen and Y. Chen, *Adv. Mater.*, 2013, **25**, 1692.
22 L. Q. Zhu, C. J. Wan, L. Q. Guo, Y. Shi and Q. Wan, *Nat. Commun.*, 2014, **5**, 3158.
23 J. Y. Mao, L. Hu, S. R. Zhang, Y. Ren, J. Q. Yang, L. Zhou, Y. J. Zeng, Y. Zhou and S. T. Han, *J. Mater. Chem. C*, 2019, **7**, 48–59.
24 H. Han, H. Yu, H. Wei, J. Gong and W. Xu, *Small*, 2019, **15**, 1900695.
25 W. He, Y. Fang, H. Yang, X. Wu, L. He, H. Chen and T. Guo, *J. Mater. Chem. C*, 2019, **7**, 12523–12531.
26 Y. H. Liu, L. Q. Zhu, P. Feng, Y. Shi and Q. Wan, *Adv. Mater.*, 2015, **27**, 5599.
27 T. Ahmed, S. Kuriakose, E. L. H. Mayes, R. Ramanathan, V. Bansal, M. Bhaskaran, S. Sriram and S. Walia, *Small*, 2019, **15**, 1900966.
28 S. Gao, G. Liu, H. L. Yang, C. Hu, Q. L. Chen, G. D. Gong, W. H. Xue, X. H. Yi, J. Shang and R. W. Li, *ACS Nano*, 2019, **13**, 2634–2642.
29 M. P. Kavanaugh, *Nature*, 2004, **431**, 752–753.
30 L. Shao, H. Wang, Y. Yang, Y. He, Y. Tang, H. Fang, J. Zhao, H. Xiao, K. Liang, M. Wei, W. Xu, M. Luo, Q. Wan, W. Hu, T. Gao and Z. Cui, *ACS Appl. Mater. Interfaces*, 2019, **11**, 12161–12169.
31 C. Zhou, J. Zhao, J. Ye, M. Tange, X. Zhang, W. Xu, K. Zhang, T. Okazaki and Z. Cui, *Carbon*, 2016, **108**, 372–380.
32 W. Xu, J. Dou, J. Zhao, H. Tan, J. Ye, M. Tange, W. Gao, W. Xu, X. Zhang, W. Guo, W. Xu, X. Zhang, W. Guo, C. Ma, T. Okazaki, K. Zhang and Z. Cui, *Nanoscale*, 2016, **8**, 4588–4598.
33 A. Di Bartolomeo, M. Rinzan, A. K. Boyd, Y. F. Yang, L. Guadagno, F. Giubileo and P. Barbara, *Nanotechnology*, 2010, **21**, 115204.
34 Y. Mu, C. Z. Zhao, Q. Lu, C. Zhao, Y. Qi, S. Lam, I. Z. Mitrovic, S. Taylor and P. R. Chalker, *AIP Conf. Proc.*, 2017, **1877**, 090004.
35 A. Di Bartolomeo, Y. Yang, M. B. M. Rinzan, A. K. Boyd and P. Barbara, *Nanoscale Res. Lett.*, 2010, **5**, 1852.
36 D. Wei, X. Zhang, R. Jia, L. Huang, X. Zhang and J. Jie, *NPG Asia Mater.*, 2019, **11**, 77.
37 M. N. Ke, M. Takenaka and S. Takagi, *IEEE J. Electron Dev.*, 2018, **6**, 950–955.
38 E. S. Fortune and G. J. Rose, *Trends Neurosci.*, 2001, **24**, 381–385.
39 J. M. Cortes, J. J. Torres, J. Marro, P. L. Garrido and H. J. Kappen, *Neural Comput.*, 2006, **18**, 614–633.
40 M. Marcus, J. Simmons, O. Castellini, R. Hamers and M. Eriksson, *J. Appl. Phys.*, 2006, **100**, 084306.
41 P. Balakrishna and M. M. De Souza, *ACS Appl. Mater. Interfaces*, 2017, **9**, 1609–1618.
42 R. Ding, X. Liao, J. C. Li, J. X. Zhang, M. Wang, Y. Guang, H. Qin, X. Y. Li, K. Zhang, S. S. Liang, J. H. Guan, J. Lou, H. B. Jia, B. B. Chen, H. Shen and X. W. Chen, *Sci. Rep.*, 2017, **7**, 2873.
43 J. R. Fetcho, K. J. A. Cox and D. M. O'malley, *Histochem. J.*, 1998, **30**, 153–167.
44 B. U. Pedroni, S. Joshi, S. R. Deissl, S. Sheik, G. Detorakis, S. Paul, C. Augustine, E. O. Neftci and G. Cauwenberghs, *Front. Neurosci.*, 2019, **13**, 357.
45 J. Cheng, X. Huang, Y. Liang, T. Xue, L. C. Wang and J. Bao, *J. Biol. Rhythms*, 2018, **33**, 65–75.